Effect of 4d transition metals on the electronic structure and magnetic properties of α-Fe

1998 J. Phys.: Condens. Matter 10 371

(http://iopscience.iop.org/0953-8984/10/2/016)

J. Phys.: Condens. Matter **10** (1998) 371–377. Printed in the UK PII: S0953-8984(98)83294-3

Effect of 4d transition metals on the electronic structure and magnetic properties of α-Fe

Tadashi Kai†, Masahide Nakamura†, Noriyuki Takano‡, Yoshiko Ohashi† and Kazuo Shiiki†

† Department of Instrumentation Engineering, Faculty of Science and Technology, Keio University, Yokohama 223, Japan

‡ Department of Mechanical Systems Engineering, Kanazawa Institute of Technology, Ishikawa 921, Japan

Received 9 April 1997, in final form 1 July 1997

Abstract. The electronic structure and magnetic properties of bcc random alloys with Fe and 4d transition metals were studied using the first-principles Korringa–Kohn–Rostoker coherent potential approximation (KKR–CPA) method. The average magnetic moments of the alloys agreed well with the experimental results. The local magnetic moment at the Fe site was enhanced in all alloys.

1. Introduction

It is well known that the average magnetic moments of randomly substituted alloys are altered when 3d, 4d and 5d transition metals are added to α-Fe [1, 2]. During the last decade, the electronic structure and magnetic properties of random alloys have been investigated, both theoretically and experimentally. In particular, the change in the magnetic moment of Fe-based 3d transition metal alloys relative to the average number of electron per atom is known as the Slater–Pauling curve [3]. Calculations for the Fe-based 3d-transition metal alloys are made systematically [4], and the Slater–Pauling curve can be confirmed using band calculations based on the local-spin-density approximation. In contrast, the complex behaviour of Fe-based 4d transition metal alloys is generally thought to reflect the average of the magnetic moments. Fe-based platinum group metal (PGM) alloys are a special case. In the case of FeRu alloys, the magnetic moment is almost the same as that of pure Fe when the Ru concentration is less than 5 at.%. When the Ru concentration exceeds 5 at.%, the magnetic moment decreases drastically. In FeRh alloys, the magnetic moment shows even larger increases, as long as the Rh concentration remains below 20 at.%. The magnetic moment of FePd alloys decreases gradually as the Pd concentration increases. In Fe–Ag alloys, the phase diagram indicates that it is completely immiscible in equilibrium solid states [5]. However, Sumiyama and Nakamura [6] found that metastable crystalline Fe–Ag solid solutions could be obtained using a sputtering technique. They reported that the magnetic moment monotonically decreases with increasing Ag concentration.

A more accurate single-site scheme for studying the electronic structure and magnetic properties of random alloys is the Korringa–Kohn–Rostoker (KKR) method, or its linearized version, the linear-muffin-tin-orbital (LMTO) method, combined with the coherent potential approximation (CPA). Jezierski calculated the electronic structure and magnetic moment

0953-8984/98/020371+07$19.50

of FeRh alloy using the LMTO–CPA method [7]. However, the band calculation has not been performed in a self-consistent field. Kobayashi *et al* studied FeRu alloys using the KKR–CPA method and clarified the reason why adding Ru to Fe barely reduces the average magnetic moment [8]. However, the electronic structure and magnetic properties of other Fe-based 4d transition metal alloys have not yet been studied in detail. In this paper, we study the electronic structure and magnetic properties of bcc $Fe_{90}X_{10}$ (X = Nb, Mo, Tc, Ru, Rh, Pd and Ag) alloys by using the first-principles KKR–CPA method based on the local-spin-density approximation.

2. Calculation method

The electronic structure and magnetic properties of FeX alloys are calculated using the first-principles KKR–CPA [9–11] method based on the local-spin-density approximation. The procedure and accuracy of this method is the same as that for Fe–Ru [8] and Ni–Ru [12] alloy calculations.

The basic concept behind the KKR–CPA method is to calculate the local electronic structure for a single pure site, which is surrounded by an effective medium representing a configuration average of all sites. According to the density-functional theory, the charge density varies in order to obtain the minimum energy for a given potential. The potential of the ith site is expressed as the variation in energy with respect to the spin densities at the ith site as follows,

$$V_i^{\uparrow(\downarrow)}(r) = -2\sum_j Z_j \frac{l}{|r-R_j|} + 2\int \mathrm{d}^3r' \frac{\rho_j(r')}{|r-r'|} + \mu_{xc}^{\uparrow(\downarrow)}[\rho_j^{\uparrow}(r), \rho_j^{\downarrow}(r)]$$
$$= \rho_i^{\uparrow}(r) + \rho_i^{\downarrow}(r) \tag{1}$$

where Z_i is the atomic number and $\mu_{XC}^{\uparrow(\downarrow)}$ is the exchange–correlation potential with its parametrization taken from Ceperley and Alder [13] and Perdew and Zunger [14]. $\rho_i^{\uparrow(\downarrow)}$ is the electronic spin density obtained from the diagonal elements of the Green function.

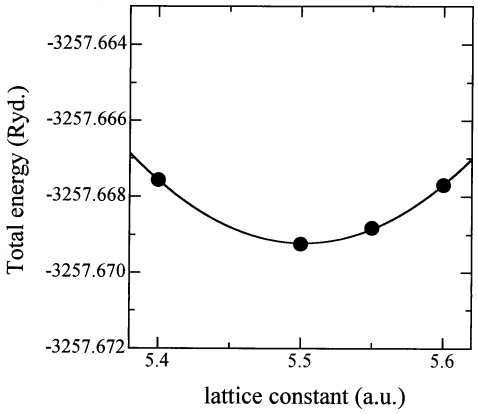

Figure 1. Total energy against lattice constant of bcc $Fe_{90}Pd_{10}$ alloy.

The expansion of the valence wave function into spherical harmonics is truncated at $l_{max} = 2$. The k-integral is calculated using the prism method. The number of k-points depends on their position on the complex energy plane. The maximum number of k-points is 1920 within the 1/48 irreducible Brillouin zone.

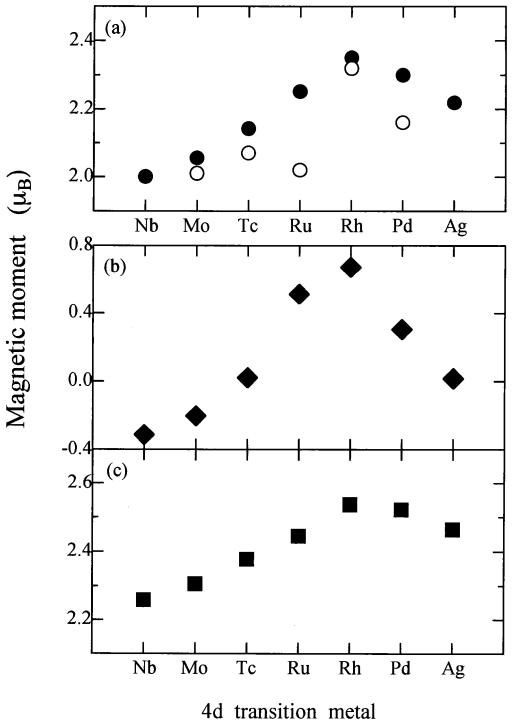

Figure 2. (a) Average magnetic moment, (b) local magnetic moment at X site and (c) local magnetic moment at Fe site in various X atoms. The solid and open circles represent values obtained by calculation and experiment, respectively.

When the electronic structure and magnetic moment of bcc $Fe_{90}X_{10}$ alloy was estimated using the KKR–CPA method, the total energy converged to less than 10^{-2} mRyd/atom. Figure 1 shows the total energy against the lattice constant of bcc $Fe_{90}Pd_{10}$ alloy. The lattice constants of these alloys were determined from the energy minimum. Among the bcc $Fe_{90}X_{10}$ alloys, only the $Fe_{90}Pd_{10}$ alloy was the subject of this [15]. The lattice constant was 5.50 au. The calculated lattice constant of the $Fe_{90}Pd_{10}$ alloy was 5.502 au, which is in good agreement with the experimental results.

3. Results and discussion

Figure 2(a) shows the average magnetic moments of bcc $Fe_{90}X_{10}$ alloys. The open and solid circles show the average magnetic moments obtained experimentally and by calculation [1, 16], respectively. The average magnetic moments are in good agreement with the experimental results except for the $Fe_{90}Ru_{10}$ alloy. As pointed out by Kobayashi *et al* [8], the discrepancy seen in the FeRu alloy is thought to arise from a change in the crystal structure. Although the FeRu alloy contains fcc and hcp structures when the Ru concentration exceeds 5 at.%, the other FeX alloys contains only bcc structure at an X concentration of less than 10 at.% [17].

Figure 2(b) shows the local magnetic moments obtained by calculation at X atom sites. The local magnetic moments of X atoms with a valence less than that of Fe are negative,

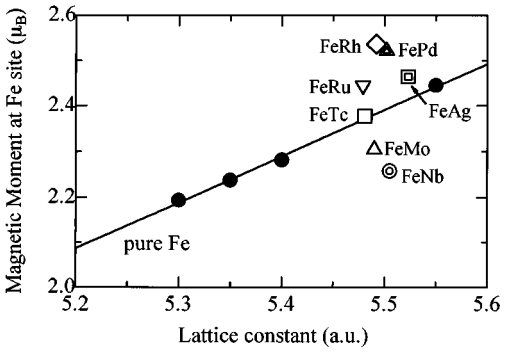

Figure 3. Relationship between lattice constants and Fe local magnetic moment for bcc $Fe_{90}X_{10}$ alloys. Solid line shows pure Fe obtained by calculation.

that is, the X atoms have local magnetic moments anti-parallel to those of the Fe moment. X atoms with valence numbers greater than Fe exhibit positive local moments. These characteristics are similar to those for transition metal impurities [18].

Figure 2(c) shows the local magnetic moments at the Fe sites. All the magnetic moments were greater than that of pure Fe (2.228 μ_B) obtained from our calculation. This behaviour differs from the results obtained when 4d impurities in Fe are calculated without lattice relaxation [18]. Changes in the calculated magnetic moments ΔM at the Fe site, the majority spin charge $\Delta Z_\uparrow$ and the minority spin charge $\Delta Z_\downarrow$ as well as the charge transferred from the X atom to the Fe site are shown in table 1. It can be seen that the change in moment was relatively small for the $Fe_{90}Nb_{10}$ alloy and is large for the $Fe_{90}Rh_{10}$ and $Fe_{90}Pd_{10}$ alloys. Conversely, the charge transfer was large for the $Fe_{90}Nb_{10}$ alloy and small for the $Fe_{90}Rh_{10}$ and $Fe_{90}Pd_{10}$ alloys. For pure Fe, the majority spin band is not fully occupied and the Fermi energy lies in the minimum range of the minority-spin density of states [18]. Therefore, it is reasonable to assume that the transferred electrons favour the majority-spin band rather than the minority-spin band. It is plausible that the charge transfer contributes to the enhanced magnetic moment as a result of occupying the majority band, although few electrons are transferred compared to the total magnetic moment, for example 2% in FeNb and 0.2% in FeRh. Kobayashi *et al* pointed out [8] that the enhanced magnetic moment at the Fe site is partly the result of the magnetovolume effect and the charge transfer for FeRu alloys. The rest of the enhanced magnetic moments can be regarded as arising from the magnetovolume effect.

Table 1. Change in calculated local magnetic moments, Fe site ΔM, the majority spin charges $\Delta Z_\uparrow$, the minority spin charges $\Delta Z_\downarrow$ and the charge transfer ΔZ from the X site to Fe in the $Fe_{90}X_{10}$ alloys.

	Nb	Mo	Tc	Ru	Rh	Pd	Ag
ΔM (μ_B)	0.030	0.077	0.149	0.217	0.309	0.294	0.236
$\Delta Z_\uparrow$	0.039	0.056	0.086	0.115	0.158	0.150	0.127
$\Delta Z_\downarrow$	0.009	−0.021	−0.063	−0.102	−0.151	−0.143	−0.110
ΔZ	0.048	0.035	0.023	0.013	0.007	0.007	0.017

Figure 3 shows the relationship between the Fe local moment and lattice constant for the bcc $Fe_{90}X_{10}$ alloy. The solid line shows the magnetic moment of pure iron obtained from

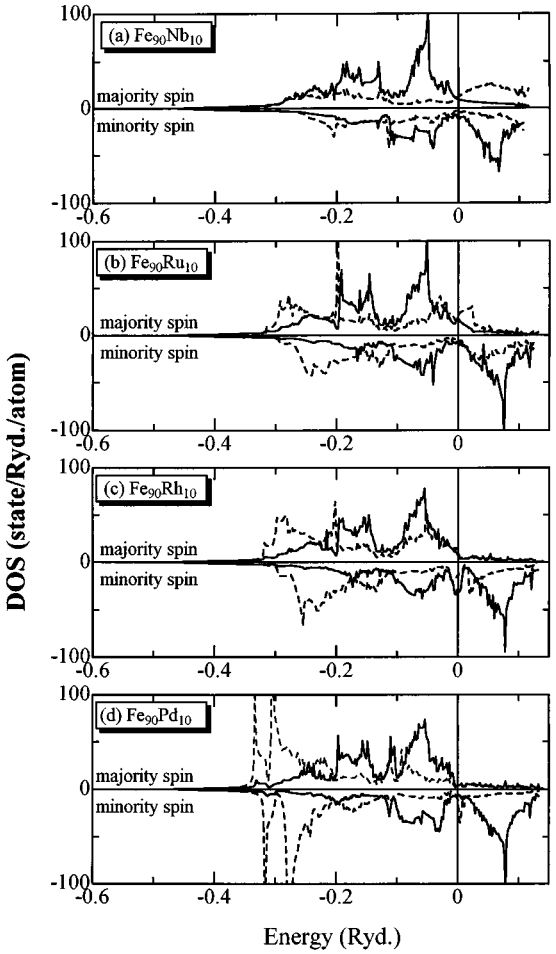

Figure 4. Density of states of (a) $Fe_{90}Nb_{10}$ alloy, (b) $Fe_{90}Ru_{10}$ alloy (c) $Fe_{90}Rh_{10}$ alloy, and (d) $Fe_{90}Pd_{10}$ alloy. Solid line shows the density of states at Fe site and dotted line shows the density of states at 4d element site.

our calculation as a function of the lattice constant. This result can generally be regarded as the magnetovolume effect. We found that changes in the Fe local moment in Fe-based late-4d-transition metal alloys were considerable when compared to those of the general magnetovolume effect. For FeNb and FeMo alloys, it is thought that the Fe local moment is reduced because the 4d site moment is anti-parallel to the Fe moment.

The density of states of $Fe_{90}Nb_{10}$, $Fe_{90}Ru_{10}$, $Fe_{90}Rh_{10}$ and $Fe_{90}Pd_{10}$ alloys is shown in figures 4(a)–(d). It can be seen that the majority band of $Fe_{90}Nb_{10}$ and $Fe_{90}Ru_{10}$ is not fully occupied. The majority band of $Fe_{90}Rh_{10}$ and $Fe_{90}Pd_{10}$ was saturated with electrons because of the large exchange splitting. The electronic structure of the Fe–X alloys changes between $Fe_{90}Ru_{10}$ and $Fe_{90}Rh_{10}$ alloys drastically, showing the transition from 'weak' to 'strong ferromagnetism'.

Figure 5 shows the bulk moduli of the $Fe_{90}X_{10}$ alloys. The bulk modulus of pure iron obtained using the present method, where X is regarded as Fe, is also shown in figure 5.

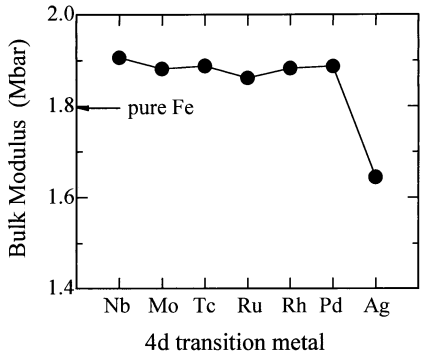

Figure 5. Bulk modulus of bcc $Fe_{90}X_{10}$ alloys. Bulk modulus of pure iron is also shown.

We found that, with the exception of the $Fe_{90}Ag_{10}$ alloy, the calculated bulk moduli of $Fe_{90}X_{10}$ alloys were larger than those of pure Fe. The bulk moduli of 4d transition metals were known to be larger than those of pure Fe [19]. Therefore enhancement of the bulk modulus can be expressed. Similarly, the bulk modulus of the $Fe_{90}Ag_{10}$ alloy was smaller than that of pure Fe because of the small bulk modulus of pure Ag (1.087 Mbar) [18].

4. Conclusion

In this paper, we clarified the electronic structure of Fe–X (X = 4d transition metal) alloys using the first-principles KKR–CPA calculation. The average magnetic moments were in good agreement with the experimental results, with the exception of the $Fe_{90}Ru_{10}$ alloy. The local magnetic moments at the Fe site were enhanced in all alloys, partly as a result of charge transfer and partly due to the magnetovolume effect. It can be concluded that the effect of the charge transfer is more pronounced for the early-4d-transition metal alloys and is relatively small for the late-4d-transition metal alloys, although the late alloys contribute somewhat to the magnetic moment. The magnetovolume effect is pronounced for the late-4d-transition metal alloys as well. As the atomic number of the X sites increases, the $Fe_{90}Rh_{10}$ alloy is transformed into a 'strong ferromagnet'.

Acknowledgments

The authors wish to acknowledge the computing support of the Keio University computer centre throughout the course of this study. This work was founded in part by a Keio University Special Grant-in-Aid for Innovative Collaborative Research Projects.

References

[1] Fallot M 1936 *Ann. Phys., Paris* **6** 305
[2] Collins M F and Forsyth J B 1963 *Phil. Mag.* **8** 401
[3] Chikazumi S 1964 *Physics of Magnetism* (New York: Wiley) p 73
[4] Drittler B, Stefanou N, Blügel S, Zeller R and Dederichs P H 1989 *Phys. Rev.* B **40** 8203
[5] Kubaschewski O 1982 *Iron-Binary Phase Diagrams* (Berlin: Springer)
[6] Sumiyama K and Nakamura Y 1984 *Phys. Status Solidi* a **81** K209
[7] Jezierski A 1993 *Solid State Commun.* **86** 685
[8] Kobayashi M, Ando N, Kai T, Takano N and Shiiki K 1995 *J. Phys.: Condens. Matter* **7** 9607

[9] Johnson D D, Nicholson D N, Pinski F J, Gyorffy B L and Stocks G M 1990 *Phys. Rev.* B **41** 9701
[10] Takano N, Oki E, Terasaki F and Fukuchi M 1993 *J. Phys.: Condens. Matter* **5** 5553
[11] Kai T, Takano N, Shiiki K and Fukuchi M 1995 *Solid State Commun.* **96** 971
[12] Kobayashi M, Kai T, Takano N, Ohashi Y and Shiiki K 1996 *J. Phys.: Condens. Matter* **8** 7863
[13] Ceperley D M and Alder B J 1980 *Phys. Rev. Lett.* **45** 566
[14] Perdew J P and Zunger A 1981 *Phys. Rev.* B **23** 5048
[15] Pearson W B 1967 *A Handbook of Lattice Spacing and Structure of Metals and Alloys* (London: Pergamon)
[16] Aldred A T 1968 *J. Phys. C: Solid State Phys.* **1** 244
[17] Shirane G, Chen C W, Flinn P A and Nathans R 1963 *Phys. Rev.* **131** 183
[18] Dederichs P H, Zeller R, Akai H and Ebert H 1991 *J. Magn. Magn. Mater.* **100** 241
[19] Moruzzi V L and Marcus P M 1993 *Phys. Rev.* B **48** 7665